water

MDPI

Article

Effect of Plastic Film Residue on Vertical Infiltration Under Different Initial Soil Moisture Contents and Dry Bulk Densities

Junhao Cao, Pengpeng Chen, Yupeng Li, Heng Fang, Xiaobo Gu * and Yuannong Li *

Key Laboratory of Agricultural Soil and Water Engineering in Arid and Semiarid Areas, Ministry of Education, Northwest A&F University, Yangling District, Xianyang 712100, China; xinongcaojunhao@163.com (J.C.); 15129248421@163.com (P.C.); yupeng_li@nwafu.edu.cn (Y.L.); fangheng8571@163.com (H.F.)

* Correspondence: guxiaobo@nwafu.edu.cn (X.G.); liyuannong@163.com (Y.L.)

Received: 22 April 2020; Accepted: 7 May 2020; Published: 9 May 2020

Abstract: In arid and semi-arid regions, plastic film mulching can effectively improve crop yield, but with the increase of service life, a lot of residual plastic film (R_{PF}) remains in the soil. The application of a R_{PF} to a soil will alter soil moisture processes, and thus, affect the soil water distribution and its effectiveness. A quadratic regression orthogonal design was used to study the effects of initial moisture content (I_{MC}), dry bulk density (D_{BD}), residual plastic film content (R_{PFC}), and the burial depth of R_{PF} on the migration time of wetting front (M_F), moisture content (M_C), and accumulative infiltration (A_I) of a test soil. It was found that I_{MC}, D_{BD}, and R_{PFC} were the main factors affecting M_C, M_F, and A_I, while the burial depth of R_{PF} had no significant influence. The order of influence for the factors affecting M_F was $I_{MC} > D_{BD} > R_{PFC}$, while the order of influence for the factors affecting M_C and A_I was $D_{BD} > I_{MC} > R_{PFC}$. R_{PFC} was parabolic in relation to M_F, M_C, and A_I, when it was in the range of 50–100 kg/hm^2, while within the same range M_C and A_I reached a maximum and M_F reached a minimum. The analysis of the interactive responses revealed that when the D_{BD} was greater than 1.29g/cm^3, the M_F initially decreased and then increased with the increase of R_{PFC}. When the R_{PFC} was more than 100 kg/hm^2, the M_F initially increased and then decreased with the increase of the D_{BD}. When the D_{BD} was larger than 1.31 g/cm^3, the A_I initially increased and then decreased with the increase of R_{PFC}. It was apparent that the R_{PF} not only had a blocking effect on the wetting front, but also affected the water flow. When the R_{PFC} was between 50 and 100 kg/hm^2, the soil M_C was significantly increased. It was suggested that the R_{PF} pollution area should increase the mechanical recovery of plastic film, standardize the use and recycling of agricultural R_{PF}, optimize the planting model, and establish a recyclable model for the treatment of R_{PF} pollution, and it was proposed that the R_{PFC} remaining after recovery of the R_{PF} should be less than 50 kg/hm^2.This study can prove the law of soil water movement in the residue film pollution area and provide reference and solution ideas for the comprehensive treatment of residue film pollution in farmland.

Keywords: residual plastic film; burial depth; moisture content; wetting front of migration time; accumulative infiltration

1. Introduction

Since the 1950s, plastic film mulching technology has been widely used agricultural production processes worldwide [1,2]. At present, there are two main methods of plastic film mulching: Surface mulching and ridge-furrow mulching [3,4]. According to the research, plastic film mulching technology can reduce soil evaporation [5,6], improve crop yield and quality [7,8], improve the surface water use efficiency in water shortage areas [9], and it can also increase the surface temperature to promote crop emergence [10]. In arid and semi-arid areas, most farmers have been using plastic film mulching technology to increase crop yield in order to increase their income [11]. Plastic film plays an important role in agriculture in arid and semi-arid areas [12].

However, with the long-term use of this technology, the accumulation of residual plastic in the soil during mulching applications has been ignored [13]. In 2014, the global use of plastic film was 1.4 million tons [14]. The agricultural use of plastic film is continuing to increase [15]. The physical and chemical properties of the cultivated soil and its nutritional status can be significantly decreased [16], seriously hindering the development of the crop root system [17,18] and its absorption and utilization of water and fertilizer [19,20]. The accumulation of residual plastic has resulted in a continuous decline of the land production capacity in areas affected by the long-term use of plastic film [19,21], restricting the sustainable development of agricultural ecosystems, causing water bodies pollution [22], and leading to the "white revolution" of mulch being referred to as "white pollution" or even a "white disaster" [23,24]. Due to a lack of environmental awareness, the problem of residual plastic film (R_{PF}) affecting soil productivity has been ignored for a long time [13,25]. In addition, to reduce production costs, the thickness of the plastic film applied has decreased in recent years, which has led to an increased incidence of film breakage, while recovery has become more difficult. The accumulation rate of R_{PF} in agricultural soils is accelerating, and the area of polluted land is expanding [26]. In the long term, the negative outcomes of plastic film pollution will gradually outweigh the economic benefits of the heat and moisture preservation [27,28]. However, the large production costs of degradable membranes make them difficult to promote [29]. Therefore, plastic film cannot currently be replaced by alternative products.

In recent years, membrane fouling as a form of "white pollution" has been taken seriously by agricultural, water conservancy, and environmental professionals [24,30,31], with most plastic film mulch research focusing on the film thickness [32], material [15], the potential for biodegradable films [13], and covering effects [33,34]. There has been less focus on the impact of R_{PF} on soil infiltration and soil water redistribution, with problems such as soil moisture availability receiving little attention. Previous studies have been conducted to investigate the influence of R_{PFC} and burial depth of R_{PF} on soil infiltration [35]. The influence of excessive applications and burial depths of R_{PF} have been considered as single factors [36] and the relationship between the soil M_C and the migration time of wetting front (M_F), and the burial depth of R_{PF}, R_{PFC}, dry bulk density (D_{BD}), and initial moisture content (I_{MC}) need to be studied in terms of their interactive effects on the M_F and their influence on soil M_C.

Therefore, this study used a quadratic regression orthogonal experimental design to: (1) Determine the influence of R_{PFC}, burial depth of R_{PF}, D_{BD}, and I_{MC} on the M_F and soil M_C; (2) determine the influence of the interactions between two factors on the M_F and soil M_C; (3) establish an optimal R_{PFC} and soil permeability, where the relationship between the plastic film and land use does not influence the production capacity of the land; and (4) determine a theoretically reasonable irrigation system in areas affected by plastic membrane pollution.

2. Materials and Methods

2.1. Experimental Site

The experiment was conducted at an experimental station (34°18′N, 108°24′E; 521 m a.s.l.) of the Key Laboratory of Agricultural Soil and Water Engineering, Ministry of Education, Northwest A & F University, located in Yangling, Shaanxi Province in northwest China. The experimental site was flat and open terrain, with abundant light and heat resources. The average sunshine per year of 2527.1h, average annual temperature of 13 °C (obtained at Yangling Meteorological Bureau). The average evaporation was 1500 mm and the groundwater depth was 80 m, with the area being classed as semi-humid and drought-prone.

2.2. Experimental Materials and Devices

Soil samples were taken from the surface of the test field in the experimental station. The texture of the soil was a loam. After removing impurities such as plant roots and stones, air drying, mechanical rolling, and passing through a 5mm screen the I_{MC} was 2.0%. Soil particle size was determined by an MS2000 laser particle size analyzer (Malvern Instruments, Malvern, UK). Clay particles (d < 0.002 mm) comprised 22.1% of the soil, fine particles (0.002 < d < 0.005mm) accounted for 5.8%, medium sized powder (0.005 < d < 0.02 mm) accounted for 26.4%, powder (0.02 < d < 0.05 mm) accounted for 37.8%, and extremely fine sand (0.05 < d < 0.25 mm) accounted for 7.93%. The saturated hydraulic conductivity and saturated soil moisture were 24.36 cm d^{-1} and 0.48 cm^3 cm^{-3}, respectively. The soil organic carbon was 6.50 g kg^{-1}. The dry bulk density of soil was 1.40 gcm^{-3}. The basic physical and chemical shape of soil was: organic matter 11.20 g kg^{-1}, total nitrogen 0.93 g kg^{-1}, nitrate nitrogen 76.27 mg kg^{-1}, available phosphorus 25.38 mg kg^{-1}, available potassium 131.97 mg kg^{-1}, PH value was 8.12.

The transparent film thickness was 0.008mm (Shandong Xifeng Plastic Industry Co., Ltd., Shandong, China). The centrifuge method is used to obtain soil hydraulic parameters for the soil moisture characteristic curve [37]. Determination of soil moisture characteristic curve (Figure 1) by CR21GII high speed constant temperature freezing centrifuge made in Japan.

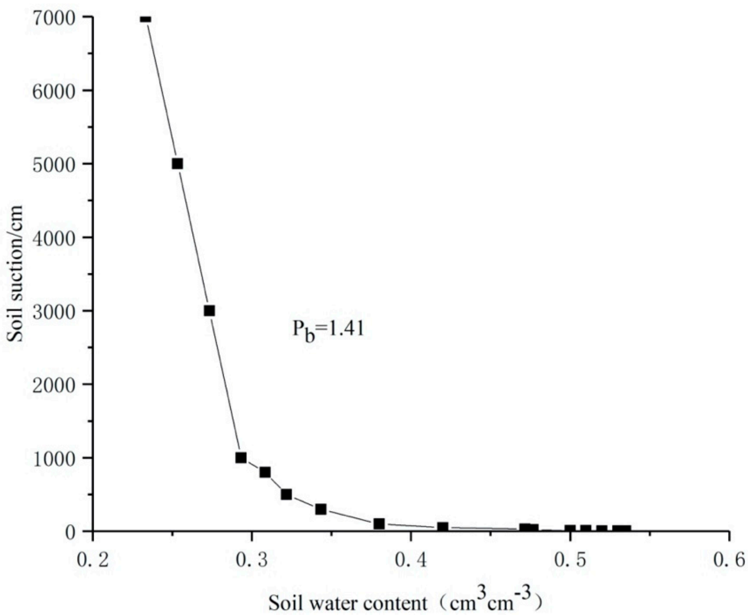

Figure 1. Soil moisture characteristic curve.

As shown in Figure 2, the test device had a Mariotte's bottle height of 70 cm, the soil column height was 60 cm, and radius (r) = 12 cm. The Mariotte's bottle and soil column were made of plexiglass. There was a water outlet at the bottom of the Mariotte's bottle at 2 cm, and a 67 cm long plexiglass pipe was placed inside. The lower end of the plexiglass tube was 6 cm higher than the soil surface in the soil column (the infiltration head was maintained constantly at 6 cm). There was an air vent at the lower end of the soil column, located 2 cm from the base. During the infiltration process, the air in the soil was discharged through the air vent to maintain the pressure balance in the infiltration process. The bottom 5 cm of the soil column was filled with quartz stone, and 5 cm of settled soil was laid on the quartz stone (to prevent the test soil sample from entering the quartz stone crack). The soil in the column was divided into four sections (0–10, 10–20, 20–30, and 30–40 cm soil layers). Two round holes (r = 1 cm) were made in the middle part of each layer to enable the measurement of soil M_C at the end of the test, and rubber plugs were used to seal the holes and prevent leakage during the experiment.

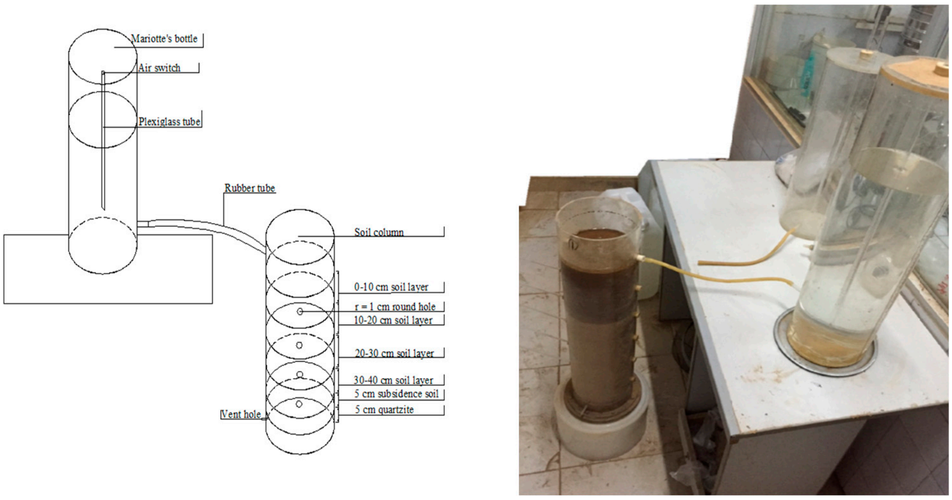

Figure 2. Schematic of the experimental design.

2.3. Design and Methods

2.3.1. Experimental Design

Four factors (I_{MC}, D_{BD}, R_{PFC}, and burial depth of R_{PF}) were selected for testing in the experiment, with each factor selected at five levels. A four-factor and five-level quadratic regression orthogonal experimental design was adopted. Each factor had five levels and a total of 36 combinations. Each combination was repeated three times and the results were averaged. The horizontal coding tables of each factor are shown in Table 1 and the experimental scheme is shown in supplementary materials.

Table 1. Test factors and levels.

Z_j	I_{MC} Z_1/%	D_{BD} Z_2/(g/cm^3)	R_{PFC} Z_3/(kg/hm^2)	Burial Depth of R_{PF} Z_4/cm
r (2)	16	1.45	200	30~40
1	14	1.41	150	20~30
0	11	1.35	100	10~20
−1	8	1.29	50	0~10
r (−2)	6	1.25	0	0

I_{MC}, D_{BD}, R_{PFC} and R_{PF} represents mean initial moisture content, dry bulk density, residual plastic film content and residual plastic film, respectively.

2.3.2. Data Analysis

When there are p variables, the general form of a quadratic regression equation is:

$$y = b_0 + \sum_{j=1}^{p} b_j x_j + \sum_{k=1}^{p-1} \sum_{j=k+1}^{p} b_{kj} x_k x_j + \sum_{j=1}^{p} b_{jj} x_j^2 \quad (1)$$

(1) Calculation of bj

$$b_0 = \frac{B_0}{n},\ b_j = \frac{B_j}{d_j},\ b_{kj} = \frac{B_{kj}}{d_{kj}},\ b_{jj} = \frac{B_{jj}}{d_{jj}} \quad (2)$$

where n denotes the number of tests,

$$d_j = \sum_{i=1}^{n} z_{ij}^2,\ d_{kj} = \sum_{i=1}^{n} \left(z_{ik} z_{ij}\right)^2,\ d_{jj} = \sum_{i=1}^{n} \left(z'_{jj}\right)^2 \quad (3)$$

(2) Calculation of B_j

$$B_0 = \sum_{i=1}^{n} y_i, B_j = \sum_{i=1}^{n} z_{ij} y_i, B_{kj} = \sum_{i=1}^{n} z_{ik} z_{ij} y_i, B_{jj} = \sum_{i=1}^{n} z'_{ij} y_i \tag{4}$$

where Z_{ik} represents the data corresponding to row i of Z_k in supplementary materials, Z'_{ik} represents the data corresponding to row i of Z'_i in supplementary materials, and y_i represents the data corresponding to row i of y in supplementary materials.

Testing of the Regression Equation

$$F = \frac{U/f_u}{Q_{e2}/f_{e2}} F(f_u, f_{e2}) \tag{5}$$

(1) The remaining sum of squares is:

$$Q_{e2} = \sum_{i=1}^{n} y_i^2 - b_0 B_0 - \sum_{j=1}^{p} b_j B_j - \sum_{k=1}^{p-1} \sum_{j=k+1}^{p} b_{kj} B_{kj} - \sum_{j=1}^{p} b_{jj} B_{jj},\ f_{e2} = n - C_{p+2}^{2} \tag{6}$$

(2) Regression square sum:

$$U = SS_T - Q_{e2},\ f_u = C_{p+2}^{2} - 1 \tag{7}$$

(3) Total sum of squares:

$$SS_T = \sum_{i=1}^{n} y_i^2 - \frac{1}{n}\left(\sum_{i=1}^{n} y_i\right)^2 \tag{8}$$

Testing of the Fitting Degree of the Equation

$$F_{Lf} = \frac{Q_{Lf}/f_{Lf}}{Q_e/f_e} F(f_u, f_{e2}) \tag{9}$$

(1) The sum of squares of errors is obtained from the zero level test results:

$$Q_e = \sum_{i=n-f_e}^{n} y_i^2 - \frac{1}{m_0}\left(\sum_{i=n-f_e}^{n} y_i^2\right)^2,\ f_e = m_0 - 1 \tag{10}$$

where, m_0 is the number of zero level tests.

(2) Loss of quasi-sum of squares:

$$Q_{Lf} = Q_{e2} - Q_e,\ f_{Lf} = f_{e2} - f_e \tag{11}$$

All data were obtained from the average of three repeated trials. The regression equation and the fitting degree of the equation were tested using the above formulas (Equations (1), (5) and (9)). Origin 8.0 was used to analyze the single factor effect, and Matlab was used to analyze the effect of interaction between the two factors.

3. Results

3.1. Analysis of the M_F

The wetting front refers to the obvious interface between the wetted part of the soil and the dry soil layer during the process of water infiltration, and it therefore indicates the state of water movement [38]. The distribution of soil water indirectly reflected the blocking effect of R_{PF} on water movement. The R_{PF} in the field blocks the soil pores and restricts soil water movement, which results in a decrease in the soil water carrying capacity and affects the movement and distribution of the moisture front.

Based on the experimental results and calculations, quadratic regression models of M_F and I_{MC}, D_{BD}, R_{PFC}, and burial depth of R_{PF} were obtained. An analysis of variance (ANOVA) of the quadratic regression models was conducted. The results are shown in Table 2. The results showed that the linear terms of I_{MC}, R_{PFC}, and D_{BD}, the quadratic terms of R_{PFC} and D_{BD}, and the interaction terms of I_{MC} and D_{BD}, D_{BD} and R_{PFC} reached significant levels (**P** < 0.01), while the other terms were not significant. A simplified regression equation (Equation (12) was obtained after eliminating the non-significant items. Because an orthogonal design was adopted and all factors were coded by non-coding, all regression coefficients were independent of each other. Therefore, the remaining factors were fixed at zero, and an equation describing the relationship between the single factor and the M_F was obtained. A diagram showing the relationship between the single factor and the M_F was constructed using Origin. The same procedure was used to determine the relationship between the two-factor interaction effect and the M_F, and a three-dimensional figure was constructed using Matlab.

Table 2. The M_F statistical analysis and analysis of variance results.

Variance Source	Sum of Squares	Degree of Freedom	Mean Square	Partial Correlation	F-Ratio	P
Z_1	430,408.2	1	430,408.2	−0.9648	282.3304	0.0001
Z_2	175,788.2	1	175,788.2	0.9197	115.3099	0.0001
Z_3	58,608.17	1	58,608.17	0.8042	38.4446	0.0001
Z_4	80.6667	1	80.6667	−0.0501	0.0529	0.8203
Z_1^2	62.3472	1	62.3472	0.0441	0.0409	0.8417
Z_2^2	14,252.35	1	14,252.35	−0.555	9.349	0.006
Z_3^2	20,234.01	1	20,234.01	0.6223	13.2727	0.0015
Z_4^2	5390.681	1	5390.681	−0.3796	3.5361	0.074
Z_1Z_2	28,392.25	1	28,392.25	−0.6856	18.6242	0.0003
Z_1Z_3	12.25	1	12.25	0.0196	0.008	0.9294
Z_1Z_4	72.25	1	72.25	0.0475	0.0474	0.8298
Z_2Z_3	37,442.25	1	37,442.25	−0.7342	24.5606	0.0001
Z_2Z_4	2652.25	1	2652.25	0.2766	1.7398	0.2014
Z_3Z_4	702.25	1	702.25	−0.1465	0.4606	0.5047
Regression	774,098.1	14	55,292.72	F2 = 36.26979		0.0001
Residual	32,014.17	21	1524.484			
Lack of fit	22,307.92	10	2230.792	F1 = 2.52813		0.0001
Error	9706.25	11	882.3864			
Sum	806,112.2	35				

From Equation (12), it can be seen that the factors affecting M_F followed the order of I_{MC} > D_{BD} > R_{PFC} (133.92 > 85.58 > 49.42). It can be seen from Figure 3 that the M_F decreased linearly with the increase of I_{MC} and the M_F increased with the increase of D_{BD}, but the growth rate decreased slowly. The M_F initially decreased and then increased with the increase of R_{PFC}, reaching a minimum when the R_{PFC} was 51kg/hm^2 (Z_3 = −0.98). It can be seen from Figure 4 that when the D_{BD} was greater than 1.29g/cm^3 (Z_2 > −1), the M_F initially decreased and then increased with the increase of R_{PFC}. When the R_{DD} of soil was less than 1.29 g/cm^3 (Z_2 < −1), the M_F increased with the increase of R_{PFC}. When the R_{PFC} was more than 100 kg/hm^2 (Z_3 > 0), the M_F initially decreased and then increased with the increase of the D_{BD}. When the R_{PFC} was less than 100 kg/hm^2 (Z_3 < 0), the M_F increased with the increase of D_{BD}.

$$Y = 441.25 - 133.92Z_1 + 85.58Z_2 + 49.42Z_3 - 21.10Z_2^2 + 25.15Z_3^2 - 42.13Z_1Z_2 - 48.38Z_2Z_3 \quad (12)$$

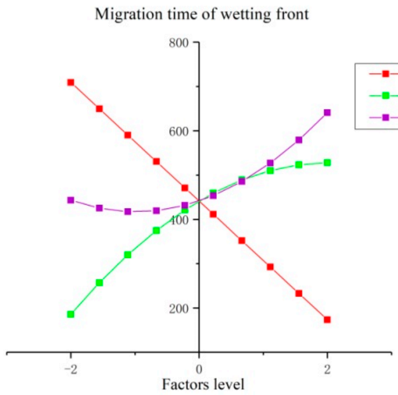

Figure 3. The relationships among M_F and various factors. Z_1, Z_2, and Z_3 represents mean initial moisture content, dry bulk density and residual plastic film content, respectively.

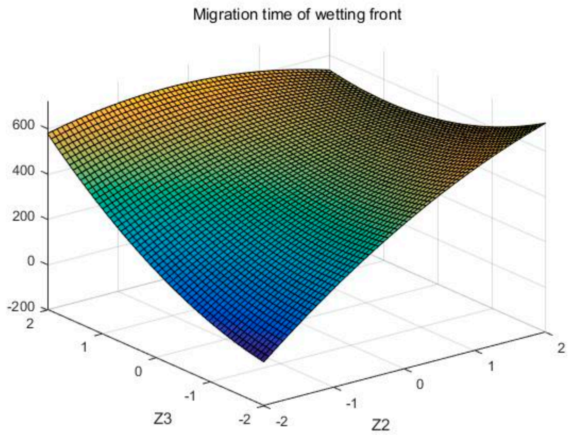

Figure 4. Surface interaction effects between D_{BD} and R_{PFC}. Z_2 and Z_3 represents mean dry bulk density and residual plastic film content respectively.

3.2. Analysis of theAccumulative Infiltration (A_I)

Accumulative infiltration refers to the total amount of water infiltrated into the soil through the surface per unit area in a certain period of time after the beginning of infiltration [39]. It can indirectly reflect the degree of blocking of soil water movement by R_{PF}. The distribution of soil water indirectly reflected the blocking effect of R_{PF} on water movement. The R_{PF} in the field blocks the soil pores, limiting soil water movement. This results in a decrease in the soil water carrying capacity and affects the movement and distribution of the moisture front. According to the analysis method described in data analysis, regression equations were obtained for A_I and I_{MC}, D_{BD}, R_{PFC}, and burial depth of R_{PF}, and an ANOVA of the regression equation was conducted, with the results shown in Table 3. After eliminating the non-significant items, the simplified regression equation shown in Equation (13) was obtained.

Table 3. The A_I statistical analysis and analysis of variance results.

Factors	Sum of Squares	Degree of Freedom	Mean Square	Partial Correlation	F-Ratio	P
Z_1	1,985,291	1	1,985,291	−0.7791	32.4444	0.0001
Z_2	13,841,432	1	13,841,432	−0.9566	226.2023	0.0001
Z_3	1,303,728	1	1,303,728	−0.7097	21.3061	0.0001
Z_4	9680.97	1	9680.97	−0.0865	0.1582	0.6948
Z_1^2	129,160.7	1	129,160.7	−0.3022	2.1108	0.161
Z_2^2	484,006.6	1	484,006.6	0.5231	7.9098	0.0104
Z_3^2	503,850.7	1	503,850.7	−0.5307	8.2341	0.0092
Z_4^2	87,288.17	1	87,288.17	−0.2522	1.4265	0.2457
Z_1Z_2	58,888.73	1	58,888.73	−0.2093	0.9624	0.3378
Z_1Z_3	104,022.4	1	104,022.4	0.2737	1.7	0.2064
Z_1Z_4	26,511.98	1	26,511.98	0.1422	0.4333	0.5175
Z_2Z_3	2,447,723	1	2,447,723	0.8098	40.0017	0.0001
Z_2Z_4	20,067.56	1	20,067.56	0.124	0.328	0.5729
Z_3Z_4	14,174.09	1	14,174.09	0.1045	0.2316	0.6353
Regression	21,015,826	14	1,501,130	F2 = 24.53208		0.0001
Residual	1,285,001	21	61,190.51			
Lack of fit	1,244,848	10	124,484.8	F1 = 34.10330		0.0001
Error	40,152.51	11	3650.228			
Sum	22,300,827	35				

By comparing the absolute values of the coefficients for each factor, the influence of each factor on the A_I was determined and was found to follow the order of DBD > IMC > R_{PFC} (759.43 > 287.61 > 233.07). The other factors were fixed to zero to obtain an equation describing the relationship between each single factor and A_I, and a diagram to highlight this was constructed with Origin (Figure 5). From Figure 5, it can be seen that the A_I decreased linearly with the increase of I_{MC} and D_{BD}, with the relationship having a negative correlation. The A_I initially increased and then decreased with the increase of $R_{PFC,}$ displaying a parabolic curve. When the R_{PFC} reached 53kg/hm^2 ($Z_3 = -0.94$), the A_I reached its maximum value. By fixing the I_{MC} at zero, an equation describing the relationship of A_I, D_{BD}, and R_{PFC} was obtained and Matlab was used to construct a three-dimensional diagram (Figure 6). The analysis of the interaction effect showed that when the D_{BD} was more than 1.31 g/cm^3 ($Z_2 = -0.69$), the A_I initially increased and then decreased with the increase of R_{PFC}. When the D_{BD} was less than 1.31 g/cm^3 ($Z_2 = -0.69$), the A_I decreased linearly with the increase of R_{PFC}.

$$Y = 5552.55 - 287.61Z_1 - 759.43Z_2 - 233.07Z_3 - 125.48Z_3^2 + 391.13Z_2Z_3 \quad (13)$$

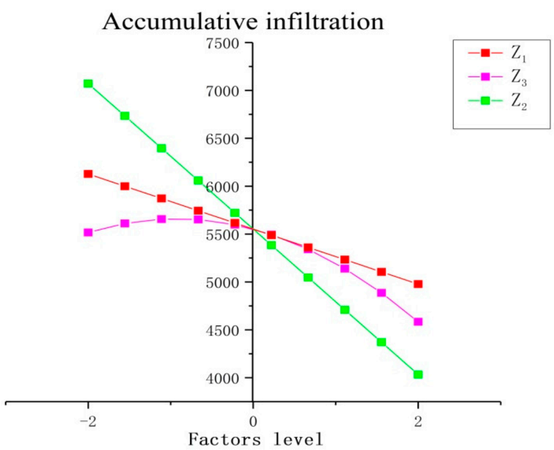

Figure 5. The relationships among A_I and various factors. Z_1, Z_2, and Z_3 represents mean initial moisture content, dry bulk density, and residual plastic film content, respectively.

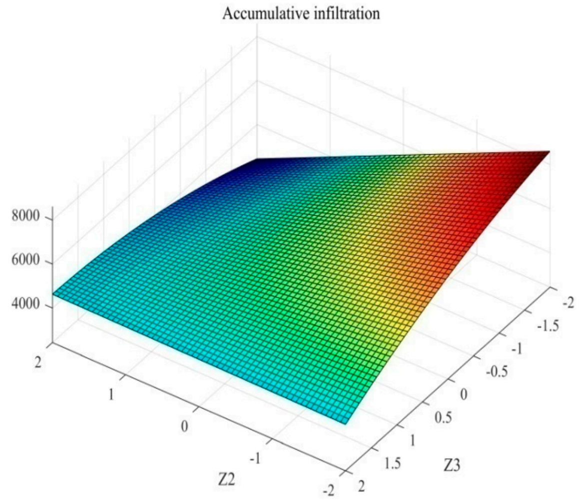

Figure 6. Surface interaction effects between D_{BD} and R_{PFC}. Z_2 and Z_3 represents mean dry bulk density and residual plastic film content respectively.

3.3. Analysis of the M_C

Soil M_C refers to the ratio of the weight of water in the soil to the weight of the corresponding solid phase material [40]. According to the analysis method used in data analysis, regression equations were obtained for M_C and I_{MC}, D_{BD}, R_{PFC}, and burial depth of R_{PF}, and an ANOVA of the regression equation was conducted, with the results shown in Tables 4–7. According to these tables, regression equations between M_C in each layer and each factor were obtained after eliminating the insignificant items (Equations (14–17)). These four equations were used to describe the relationship between the M_C in each layer and each factor (Figure 7). It can be seen from the figure that the M_C in the four layers declined linearly with the increase in I_{MC} and D_{BD}, with the relationships having a negative correlation. With the increase of R_{PFC}, the M_C initially increased and then decreased. In the 0–10cm layer, when the R_{PFC} was 74kg/hm^2 ($Z_3 = -0.52$), the M_C reached a maximum. In the layer 10–20cm, when the R_{PFC} was 68kg/hm^2 ($Z_3 = -0.64$), the M_C reached a maximum. In the 20–30cm layer, when the R_{PFC} was 71kg/hm^2 ($Z_3 = -0.58$), the M_C reached a maximum. In the 30–40cm layer, when the R_{PFC} was 59kg/hm^2 ($Z_3 = -0.82$), the M_C reached a maximum. There was no significant effect of burial depth of R_{PF} on soil M_C, and there was no interaction between the two factors.

$$Y(0\text{-}10cm) = 31.87 - 1.30Z_1 - 1.81Z_2 - 0.46Z_3 - 0.44Z_3^2 \quad (14)$$

$$Y(10\text{-}20cm) = 31.09 - 1.32Z_1 - 2.06Z_2 - 0.56Z_3 - 0.44Z_3^2 \quad (15)$$

$$Y(20\text{-}30cm) = 29.77 - 1.02Z_1 - 2.04Z_2 - 0.58Z_3 - 0.50Z_3^2 \quad (16)$$

$$Y(30\text{-}40cm) = 26.09 - 1.02Z_1 - 1.67Z_2 - 0.61Z_3 - 0.37Z_3^2 \quad (17)$$

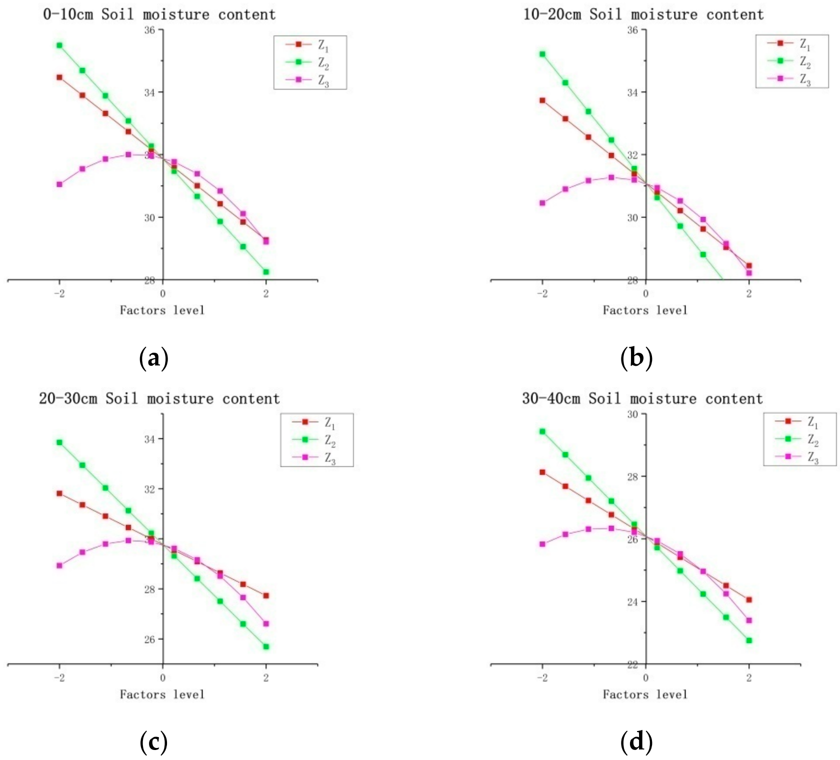

Figure 7. The relationships among M_C and various factors. Z_1, Z_2, and Z_3 represents mean initial moisture content, dry bulk density, and residual plastic film content, respectively; (**a**) The relationships among 0–10cm MC and various factors,(**b**) The relationships among 10–20cm MC and various factors, (**c**) The relationships among 20–30cm MC and various factors, (**d**) The relationships among 30–40cm MC and various factors.

Table 4. The 0–10 cm M_C statistical analysis and analysis of variance results.

Factors	Sum of Squares	Degree of Freedom	Mean Square	Partial Correlation	F-Ratio	P
Z_1	40.3782	1	40.3782	−0.89	79.9942	0.0001
Z_2	78.9525	1	78.9525	−0.939	156.4148	0.0001
Z_3	5.0508	1	5.0508	−0.5681	10.0063	0.0047
Z_4	0.0002	1	0.0002	−0.0044	0.0004	0.9841
${Z_1}^2$	0.0458	1	0.0458	0.0656	0.0906	0.7663
${Z_2}^2$	3.8157	1	3.8157	0.5145	7.5594	0.012
${Z_3}^2$	6.1864	1	6.1864	−0.6071	12.256	0.0021
${Z_4}^2$	2.2103	1	2.2103	0.4154	4.3788	0.0487
Z_1Z_2	0.8236	1	0.8236	0.2685	1.6316	0.2154
Z_1Z_3	0.6765	1	0.6765	−0.2449	1.3402	0.26
Z_1Z_4	2.4571	1	2.4571	−0.4338	4.8677	0.0386
Z_2Z_3	1.8701	1	1.8701	0.3873	3.7048	0.0679
Z_2Z_4	0.2377	1	0.2377	−0.1481	0.4708	0.5001
Z_3Z_4	1.2939	1	1.2939	−0.3298	2.5634	0.1243
Regression	143.9986	14	10.2856	F2 = 20.37708		0.0001
Residual	10.6	21	0.5048			
Lack of fit	10.3697	10	1.037	F1 = 49.52981		0.0001
Error	0.2303	11	0.0209			
Sum	154.5987	35				

Table 5. The 10–20cm M_C statistical analysis and analysis of variance results.

Factors	Sum of Squares	Degree of Freedom	Mean Square	Partial Correlation	F-Ratio	P
Z_1	41.554	1	41.554	−0.851	55.1587	0.0001
Z_2	102.0113	1	102.0113	−0.9304	135.4094	0.0001
Z_3	7.5264	1	7.5264	−0.5678	9.9905	0.0047
$Z4$	0.1442	1	0.1442	−0.095	0.1913	0.6663
$Z_1{}^2$	1.4706	1	1.4706	0.2916	1.9521	0.177
$Z_2{}^2$	0.5778	1	0.5778	0.1877	0.767	0.3911
$Z_3{}^2$	6.2481	1	6.2481	−0.5321	8.2937	0.009
$Z_4{}^2$	0.3828	1	0.3828	0.1537	0.5081	0.4838
Z_1Z_2	0.6241	1	0.6241	0.1948	0.8284	0.3731
Z_1Z_3	1.092	1	1.092	−0.2541	1.4496	0.242
Z_1Z_4	1.199	1	1.199	−0.2654	1.5916	0.2209
Z_2Z_3	1.3924	1	1.3924	0.2844	1.8483	0.1884
Z_2Z_4	0.0625	1	0.0625	−0.0627	0.083	0.7761
Z_3Z_4	0.7656	1	0.7656	−0.2149	1.0163	0.3249
Regression	165.0509	14	11.7893	F2 = 15.64914		0.0001
Residual	15.8204	21	0.7534			
Lack of fit	14.5316	10	1.4532	F1 = 12.40190		0.0001
Error	1.2889	11	0.1172			
Sum	180.8713	35				

Table 6. The 20–30cm M_C statistical analysis and analysis of variance results.

Factors	Sum of Squares	Degree of Freedom	Mean Square	Partial Correlation	F-Ratio	P
Z_1	24.8067	1	24.8067	−0.7409	25.5609	0.0001
Z_2	99.5523	1	99.5523	−0.9111	102.5792	0.0001
Z_3	7.958	1	7.958	−0.5299	8.2	0.0093
$Z4$	0.028	1	0.028	−0.0371	0.0289	0.8667
$Z_1{}^2$	0.091	1	0.091	0.0667	0.0938	0.7624
$Z_2{}^2$	0.9614	1	0.9614	0.2122	0.9907	0.3309
$Z_3{}^2$	7.854	1	7.854	−0.5274	8.0928	0.0097
$Z_4{}^2$	0.2568	1	0.2568	0.1116	0.2646	0.6123
Z_1Z_2	0.6006	1	0.6006	0.1692	0.6189	0.4402
Z_1Z_3	0.0042	1	0.0042	0.0144	0.0044	0.948
Z_1Z_4	0.5256	1	0.5256	−0.1586	0.5416	0.4699
Z_2Z_3	1.113	1	1.113	0.2276	1.1469	0.2964
Z_2Z_4	3.441	1	3.441	−0.3801	3.5457	0.0736
Z_3Z_4	0.3906	1	0.3906	−0.1371	0.4025	0.5327
Regression	147.5834	14	10.5417	F2 = 10.86219		0.0001
Residual	20.3803	21	0.9705			
Lack of fit	19.9954	10	1.9995	F1 = 57.14589		0.0001
Error	0.3849	11	0.035			
Sum	167.9637	35				

Table 7. The 30–40cm M_C statistical analysis and analysis of variance results.

Factors	Sum of Squares	Degree of Freedom	Mean Square	Partial Correlation	F-Ratio	P
Z_1	24.9492	1	24.9492	−0.8376	49.3765	0.0001
Z_2	67.0338	1	67.0338	−0.9292	132.6653	0.0001
Z_3	8.9426	1	8.9426	−0.6763	17.6981	0.0004
$Z4$	0.0925	1	0.0925	−0.093	0.1831	0.6731
$Z_1{}^2$	1.2813	1	1.2813	0.3282	2.5359	0.1262
$Z_2{}^2$	3.3822	1	3.3822	0.4916	6.6936	0.0172
$Z_3{}^2$	4.4377	1	4.4377	−0.543	8.7826	0.0074
$Z_4{}^2$	2.858	1	2.858	0.4606	5.6563	0.027
Z_1Z_2	0.5006	1	0.5006	0.2122	0.9906	0.3309
Z_1Z_3	0.6521	1	0.6521	−0.2406	1.2905	0.2688
Z_1Z_4	1.9113	1	1.9113	−0.3907	3.7826	0.0653
Z_2Z_3	0.015	1	0.015	0.0376	0.0297	0.8648
Z_2Z_4	3.3948	1	3.3948	−0.4923	6.7186	0.017
Z_3Z_4	0.1351	1	0.1351	−0.1121	0.2673	0.6106
Regression	119.5862	14	8.5419	F2 = 16.90505		0.0001
Residual	10.611	21	0.5053			
Lack of fit	10.5042	10	1.0504	F1 = 108.22336		0.0001
Error	0.1068	11	0.0097			
Sum	130.1972	35				

4. Discussion

4.1. Burial Depth of R_{PF}

The burial depth of R_{PF} had little effect on the M_F, A_I, and soil M_C ($P < 0.01$), and had no significant effect on the results. However, some studies have pointed out that the burial depth of R_{PF} in the soil had a large influence on the water infiltration wetting front [41], and there was a significant difference between the movement of the wetting front in the 0–10 and 10–20 cm soil layers [42]. This might be due to the fact that the water head is subject to a certain gravity effect under a certain water head (the constant water head was 6 cm in the present study), and the infiltration process occurs under a state of constant soil air pressure. The M_F was rapid, with the slowest time being 720min when the wetting front moved down to 40 cm, with the result that there was no significant effect of the burial depth of R_{PF} on the M_F. Due to the small range of R_{PFC} values (0–200 kg/hm^2) and the fast infiltration rate, the burial depth of R_{PF} did not significantly affect the soil M_C and A_I. Therefore, in the planting area where the infiltration rate of the water is faster, the influence of the buried depth of the residual film on the infiltration can be ignored for the time being.

4.2. The R_{PFC}

When the R_{PFC} was <51 kg/hm^2, the M_F decreased with the increase in R_{PFC}, which was conducive to the downward movement of water. When the R_{PFC} was greater than 51 kg/hm^2, the M_F increased with the increase in R_{PFC}, which had a blocking effect on the downward movement of the wetting front in the soil [16]. Most previous studies have shown that the R_{PFC} only had a blocking effect on water transport. In the present study, when the R_{PFC} was <51 kg/hm^2, the distribution of R_{PF} in the soil was relatively scattered, and R_{PF} was present in various forms such as sheets, rods, balls, and cylinders. When water flowed over the R_{PF}, the smooth surface of the plastic film formed a smooth diversion surface, enabling water to move rapidly downward. When the R_{PFC} was >51kg/hm^2, there were many molecular chain branches within the R_{PF}. After encountering water, the adsorption capacity of the adjacent R_{PF} increased, reducing the number of rapid water transport channels and the cross-sectional area of the soil water. The air pressure of the interface between R_{PF} and soil particles increased with the increase in the amount of infiltration water [43]. A narrow wet area could then easily form at the front of the R_{PF} due to the presence of the different large non-uniform flow fields. The soil in the wet area could not achieve a water balance with other areas, in which a water balance is driven by the matrix potential in the short-term. This reduced the driving effect of the matrix potential on the soil water and enhanced the blocking effect of the R_{PF} on soil water movement. This observation was similar to the results of previous studies obtained by adding other mulches.

The relationship between the R_{PFC} and A_I was described by a parabola (a < 0). When the R_{PFC} was 53 kg/hm^2, A_I reached its maximum value. This was because when the R_{PFC} was less than 53 kg/hm^2, the water transfer rate was faster with an increase in the R_{PFC}, which led to a gradual increase in A_I. When the R_{PFC} was >53 kg/hm^2, the R_{PF} formed an isolation layer in the soil, which destroyed the uniformity of the soil texture and its configuration, changed the soil water potential at the interface between the R_{PF} and the soil, reduced the number of macropores in the soil, and reduced the soil water carrying capacity. As a result, the blocking effect of R_{PF} on the horizontal movement of soil water gradually increased, and then A_I gradually decreased with an increase in R_{PFC}.

The results show that the water content of each soil layer (0–10, 10–20, 20–30, 30–40cm) could be described by a parabolic relationship with the R_{PFC}, where α <0, with maximum values of 74, 68, 71, and 59 kg/hm^2, respectively. When the R_{PFC} was 50–100 kg/hm^2, the water content of each soil layer reached a maximum. There may be some experimental error in this test because when the water content of each layer was at a maximum the maximum R_{PFC} was not consistent, but all values were within the range of 50–100 kg/hm^2.

4.3. The $I_{MC}$and D_{BD}

With an increase in the I_{MC}, the M_F, A_I, and soil M_C all decreased linearly. This was because the higher the I_{MC} of the soil, which could degrade the effectiveness of soil infiltration and permeability [12], resulting in less A_I. For the same infiltration time less water was able to infiltrate soils with a higher I_{MC}, and therefore, the M_F was shorter and the water M_C decreased accordingly.

The D_{BD} of the soil was positively correlated with the M_F, and negatively correlated with A_I and M_C. This was because the larger the D_{BD}, the smaller the pores between the soil particles, the greater the blocking effect on soil water migration, and fewer water molecules can be contained in the soil. The D_{BD} was therefore positively related to the M_F and negatively related to the A_I and M_C. However, with an increase in the D_{BD}, the porosity of the soil decreased and the influence of D_{BD} on soil infiltration was reduced. This resulted in a decrease in the advance of the wetting front.

4.4. Interaction Effects Between Two Factors

The analysis of the interaction between two factors showed that when the D_{BD} of soil was <1.29 g/cm^3, with an increase in the R_{PFC} the M_F increased. When the D_{BD} of soil was >1.29 g/cm^3, with an increase in the R_{PFC}, the M_F initially decreased and then increased. When the D_{BD} was >1.31 g/cm^3, the A_I initially increased and then decreased with an increase in the R_{PFC}. When the D_{BD} was <1.31 g/cm^3, the A_I decreased linearly with an increase in the R_{PFC}. This was because the soil D_{BD} was small and the soil porosity was large, with the shape of the R_{PF} being more irregular in soil with a small D_{BD} than in soil with a large D_{BD}. The R_{PF} isolation layer destroyed the capillary connectivity of the soil, blocked the continuity of the soil pore connectivity and the water transmission capacity, reduced the vertical infiltration capacity of the soil water, and caused the soil water movement to slow down, which influenced the A_I. When the D_{BD} was large and the R_{PFC} was small, the soil porosity was small, and a dense blocking layer formed between the soil particles. A lower R_{PFC} could form a surface to guide the flow of water, which would promote the infiltration of soil water and reduce the M_F, which would lead to an increase in the A_I. When the R_{PFC} was <100 kg/hm^2, the M_F increased with the increase of D_{BD}. When the R_{PFC} was more than 100 kg/hm^2, the M_F changed to a lesser extent with the increase in R_{PFC}. This was because when the R_{PFC} was large, the D_{BD} of the soil was low and the R_{PF} had a blocking effect on soil water movement. When the D_{BD} of the soil increased the adsorption capacity between adjacent pieces of R_{PF} decreased, but still had a guiding role.

This study analyzed the influence of various factors on the M_F, A_I, and M_C. These three factors were all fixed to zero for analysis, while the I_{MC} was 11%, the D_{BD} of the soil was 1.35 g/cm^3, and the R_{PFC} was 100kg/hm^2. Through an analysis of the interaction effect between two factors, it was found that changes in the D_{BD} and R_{PFC} had a certain influence on the result when the magnitude of the factors was fixed to zero. Through the above analysis, it was determined that the R_{PF} not only had a blocking effect on water movement, but also had a diversion effect. The influence of the R_{PFC} on soil water movement was determined through the simulation of 1 × 2 cm rectangular pieces of R_{PF}; hence, ignoring the actual differences in the shape and size of R_{PF}. In future studies, the influence of the size and shape of R_{PF} on soil hydrodynamic properties should be considered.

5. Conclusions

In arid and semi-arid areas, the amount of R_{PF} used as a mulch in farmland is increasing annually. The amount of R_{PF} in the soil is also increasing annually. The R_{PF} retained in the soil causes "white pollution" and damages the environment. In this experiment, the surface soil of Yangling was used to determine the effect of residual film on one-dimensional soil infiltration. Found that when the R_{PFC} was 50–100 kg hm^2, the M_F can reach a minimum value, and the soil M_C and A_I can reach a maximum value. There may be a certain error in the test, resulting in R_{PFC} in the range of 50–100 kg hm^{-2}. Therefore, it is proposed that the R_{PFC} should be controlled to be below 50 kg/hm^2 when the R_{PF} is recovered after agricultural operations. This study can provide a reference for reasonable irrigation in residual film area.

In the future studies, the choice of soil should be more extensive to understand the effect of R_{PFC} on infiltration. The relationship between various physiological indexes of crops and R_{PFC} should also be studied to establish a model of R_{PF} and crops yield to provide advice for the cultivation of residual film area.

Supplementary Materials: The following are available online at http://www.mdpi.com/2073-4441/12/5/1346/s1, Table S1: Quadratic regression orthogonal design and experimental results.

Author Contributions: Methodology, J.C., P.C. and Y.L.; resources, Y.L. and X.G.; data curation, J.C. and P.C.; writing—original draft preparation, J.C.; writing—review and editing, J.C.; visualization, J.C. and H.F.; supervision, L.Y.; project administration, X.G. and Y.L.; funding acquisition, J.C. All authors have read and agreed to the published version of the manuscript.

Funding: This study was supported by the National Natural Science Foundation of China (No. 51909221), the Natural Science Basic Research Plan in Shaanxi Province of China (No. 2020JQ-276), the China Postdoctoral Science Foundation (No. 2019M650277) and the Fundamental Research Funds for the Central Universities (No. 2452018089).

Conflicts of Interest: The authors declare no conflict of interest.

References

1. Lament, W.J. Plastic mulches for the production of vegetable crops. In *A Guide to the Manufacture Performance and Potential of Plastics in Agriculture*; Elsevier: Amsterdam, The Netherlands, 2017; pp. 45–60.
2. Lamont, W.J. Plastics: Modifying the microclimate for the production of vegetable crops. *Hort. Technol.* **2005**, *15*, 477–481. [CrossRef]
3. Gan, Y.T.; Siddique, K.H.M.; Turner, N.C.; Li, X.G.; Niu, J.Y.; Yang, C.; Liu, L.P.; Chai, Q. Ridge-Furrow Mulching Systems-An Innovative Technique for Boosting Crop Productivity in Semiarid Rain-Fed Environments. *Adv. Agro.* **2013**, *118*, 429–476.
4. Gu, X.B.; Li, Y.N.; Du, Y.D. Effects of ridge-furrow film mulching and nitrogen fertilization on growth, seed yield and water productivity of winter oilseed rape (Brassica napus L.) in Northwestern China. *Agric. Water Manag.* **2018**, *200*, 60–70. [CrossRef]
5. Enrique, G.S.; Braud, I.; Jean-Louis, T.; Michel, V.; Pierre, B.; Jean-Christophe, C. Modelling heat and water exchanges of fallow land covered with plant-residue mulch. *Agricul. Forest Meteorol.* **1999**, *97*, 151–169. [CrossRef]

6. Gu, X.B.; Li, Y.N.; Du, Y.D. Optimized nitrogen fertilizer application improves yield, water and nitrogen use efficiencies of winter rapeseed cultivated under continuous ridges with film mulching. *Ind. Crops Prod.* **2017**, *109*, 233–240. [CrossRef]
7. Kasirajan, S.; Ngouajio, M. Polyethylene and biodegradable mulches for agri-cultural applications: A review. *Agron. Sustain. Dev.* **2012**, *32*, 501–529. [CrossRef]
8. Gu, X.B.; Cai, H.J.; Du, Y.D.; Li, Y.N. Effects of film mulching and nitrogen fertilization on rhizosphere soil environment, root growth and nutrient uptake of winter oilseed rape in northwest China. *Soil Till. Res.* **2019**, *187*, 194–203. [CrossRef]
9. Ma, D.D.; Chen, L.; Qu, H.C.; Wang, L.Y.; Misselbrook, T.; Jiang, R. Impacts of plastic film mulching on crop yields, soil water, nitrate, and organic carbon in Northwestern China: Ameta-analysis. *Agric. Water Manag.* **2018**, *202*, 166–173. [CrossRef]
10. O'Loughlin, J.; Finnan, J.; Mcdonnell, K. Accelerating early growth in miscanthus with the application of plastic mulch film. *Biomass Bioenergy.* **2017**, *100*, 52–61. [CrossRef]
11. Daryanto, S.; Wang, L.X.; Jacinthe, P.A. Can ridge-furrow plastic mulching replace irrigation in dryland wheat and maize cropping systems? *Agricul. Water Manag.* **2017**, *190*, 1–5. [CrossRef]
12. Al-Shammary, A.A.G.; Kouzani, A.; Gyasi-Agyei, Y.; Gates, W.; Rodrigo-Comino, J. Effects of solarisation on soil thermal-physical properties under different soil treatments: A review. *Geoderma* **2020**, *363*, 114137. [CrossRef]
13. Yang, N.; Sun, Z.X.; Feng, L.S.; Zheng, M.Z.; Chi, D.C.; Meng, W.Z.; Hou, Z.Y.; Bai, W.; Li, K.Y. Plastic film mulching for water-efficient agricultural applications and degradable films materials development research. *Adv. Manuf. Process.* **2015**, *30*, 143–154. [CrossRef]
14. Yan, C.; He, W.; Xue, Y.; Liu, Q. Application of biodegradable plastic film to reduce plastic film residual pollution in Chinese agriculture. *Chinese J. Biotechnol.* **2016**, *32*, 748–760.
15. Picuno, P. Innovative material and improved technical design for a sustainable exploitation of agricultural plastic film. *Polym. Plast. Technol. Eng.* **2014**, *53*, 1000–1011. [CrossRef]
16. Li, Y.Q.; Zhao, C.X.; Yan, C.R.; Mao, L.L.; Liu, Q.; Li, Z.; He, W.Q. Effects of agricultural plastic film residues on transportation and distribution of water and nitrate in soil. *Chemosphere.* **2020**, *242*, 125131.
17. Brodhagen, M.; Goldberger, J.R.; Hayes, D.G.; Inglis, D.A.; Marsh, T.L.; Miles, C. Policy considerations for limiting unintended residual plastic in agricultural soils. *Environ. Sci. Policy.* **2017**, *69*, 81–84. [CrossRef]
18. Guo, B.Y.; Meng, J.; Wang, X.Y.; Yin, C.N.; Hao, W.Y.; Ma, B.W.; Tao, Z. Quantification of pesticide residues on plastic mulching films in typical farmlands of the north China. *Front. Env. Eng.* **2019**, *14*. [CrossRef]
19. Zou, X.Y.; Niu, W.Q.; Liu, J.J.; Li, Y.; Liang, B.H.; Guo, L.L.; Guan, Y.H. Effects of residual mulch film on the growth and fruit quality of tomato (Lycopersicon esculentummill.). *Water Air Soil Pollut.* **2017**, *228*, 71. [CrossRef]
20. Chen, Y.S.; Wu, C.F.; Zhang, H.B.; Lin, Q.Y.; Hong, Y.W.; Luo, Y.M. Empirical estimation of pollution load and contamination levels of phthalate esters in agricultural soils from plastic film mulching in China. *Environ. Earth Sci.* **2013**, *70*, 239–247. [CrossRef]
21. Gao, H.H.; Yan, C.R.; Liu, Q.; Chen, B.Q.; Li, Z. Effects of plastic mulching and plastic residue on agricultural production: A meta-analysis. *Sci. Total Environ.* **2018**, *651*, 484–492. [CrossRef]
22. Qiuyan, Y.; Richard, S.; Jan, O. Poly hydroxyl butyrate production from municipal wastewater activated sludge with different carbon sources. *Air Soil Water Res.* **2015**, 853–858. [CrossRef]
23. Ibarra-Jiménez, L.; Lira-Saldivar, R.H.; Valdez-Aguilar, L.A.; Lozano-Del Rio, J. Colored plastic mulches affect soil temperature and tuber production of potato. *Acta Agricul. Scandinav. Sect. b-Soil Plant Sci.* **2011**, *61*, 365–371. [CrossRef]
24. Liu, E.K.; He, W.Q.; Yan, C.R. 'White revolution' to 'white pollution'—Agricultural plastic film mulch in China. *Environ. Res. Lett.* **2014**, *9*, 091001. [CrossRef]
25. Zhang, D.; Ng, E.L.; Hu, W.L.; Wang, H.Y.; Galaviz, P.; Yang, H.; Sun, W.; Li, C.; Ma, X.; Fu, B.; et al. Plastic pollution in croplands threatens long-term food security. *Global Chang. Biol.* **2020**. [CrossRef]
26. Shi, M.; Sun, Y.Y.; Wang, Z.H.; He, G.; Quan, H.X.; He, H.X. Plastic film mulching increased the accumulation and human health risks of phthalate esters in wheat grains. *Environ. Poll.* **2019**, *250*, 1–7. [CrossRef] [PubMed]

27. Gu, X.B.; Li, Y.N.; Du, Y.D. Biodegradable film mulching improves soil temperature, moisture and seed yield of winter oilseed rape (Brassica napus L.). *Soil Till. Res.* **2017**, *171*, 42–50. [CrossRef]
28. Ren, X.L.; Chen, X.L.; Cai, T.; Wei, T.; Wu, Y.; Ali, S.; Zhang, P.; Jia, Z.K. Effects of ridge-furrow system combined with different degradable mulching materials on soil water conservation and crop production in semi-humid areas of China. *Front. Plant Sci.* **2017**, *8*, 1877. [CrossRef]
29. Chiellini, E.; Cinelli, P.; D'Antone, S.; Ilieva, V.I. Environmentally degradable polymeric materials (edpm) in agricultural applications—An overview. *Polimery.* **2002**, *47*, 538–544. [CrossRef]
30. Abidli, S.; Antunes, J.C.; Ferreira, J.L.; Lahbib, Y.; Sobral, P.; El Menif, N.T. Micro plastics in sediments from the littoral zone of the north Tunisian coast (Mediterranean Sea). *Estuarine Coastal Shelf Sci.* **2018**, *205*, 1–9. [CrossRef]
31. Han, W.; Ren, J.Y.; Xuan, H.Y.; Ge, L.Q. Controllable degradation rates, antibacterial, free-standing and highly transparent films based on polylactic acid and chitosan. *Colloids Surf. A Physicochem. Eng. Asp.* **2018**, *514*, 128–136. [CrossRef]
32. Hazarika, P.; Chowdhury, D.; Chattopadhyay, A. Fabrication of submicron scale patterned plastic thin film fluidic devices with controllable thickness. *Lab Chip* **2003**, *3*, 128. [CrossRef] [PubMed]
33. Liu, Q.F.; Chen, Y.; Liu, Y.; Wen, X.X.; Liao, Y.C. Coupling effects of plastic film mulching and urea types on water use efficiency and grain yield of maize in the Loess Plateau, China. *Soil Till. Res.* **2016**, *157*, 1–10. [CrossRef]
34. Gong, D.Z.; Hao, W.P.; Mei, X.R.; Gao, X.; Liu, Q.; Caylor, K. Warmer and wetter soil stimulates assimilation more than respiration in rainfed agricultural ecosystem on the China Loess Plateau: The role of partial plastic film mulching tillage. *PlosOne.* **2015**, *10*, e0136578. [CrossRef] [PubMed]
35. Li, X.; Shi, H.; Ye, L.; Wang, Z.; Lin, Y.; Xin, L. Effects of different residual plastic film quantities in soil on drip infiltration and its uncertainty analysis. *Trans. Chin. Soc. Agric. Eng.* **2013**, *29*, 84–90, (In Chinese with English abstract).
36. Zou, X.; Niu, W.; Liu, J.; Xu, J.; Zhang, M.; Li, Y. Ability of Retarding Water Horizontal Movement for Residual Plastic Film Mixed in Soil. *J. Soil Water Conserv.* **2016**, *30*, 96–102, 108, (In Chinese with English abstract).
37. Xing, X.G.; Li, Y.B.; Ma, X.Y. Water retention curve correction using changes in bulk density during data collection. *Eng. Geol.* **2018**, *233*, 231–237. [CrossRef]
38. Bauters, T.W.J.; DiCarlo, D.A.; Steenhuis, T.S.; Parlange, J.Y. Soil water content dependent wetting front characteristics in sands. *J. Hydrol.* **2000**, *231*, 244–254. [CrossRef]
39. Fan, Y.W.; Huang, N.; Gong, J.G.; Shao, X.X.; Zhang, J.; Zhao, T. A simplified infiltration model for predicting cumulative infiltration during vertical line source irrigation. *Water.* **2018**, *10*, 89. [CrossRef]
40. Lekshmi, S.U.S.; Singh, D.N.; Baghini, M.S.A. critical review of soil moisture measurement. *Measurement* **2014**, *54*, 92–105.
41. Wang, Z.C.; Li, X.Y.; Shi, H.B.; Lin, Y.X.; Li, X.; Liang, J.C. Study on effect of plastic film residue at different buried depths on silt loam drip infiltration. *Soils.* **2014**, *46*, 710–715, (In Chinese with English abstract).
42. Li, Y.; He, Q.; Yan, C. Effect of residual film on soil infiltration under drip irrigation. *Trans. Chin. Soc. Agric. Eng.* **2015**, *31*, 145–149, (In Chinese with English abstract).
43. Grismer, M.E.; Orang, M.N.; Clausnitzer, V.; Kinney, K. Effects of air compression and counter flow on infiltration into soils. *J. Irrig. Drainage Eng.* **1994**, *120*, 775–795. [CrossRef]